International Journal of Thermodynamics (IJoT)
ISSN 1301-9724 / e-ISSN 2146-1511
https://dergipark.org.tr/en/pub/ijot

Vol. 25 (No. 2), pp. 050-062, 2022
doi: 10.5541/ijot.1017342
Published online: June 1, 2022

A Residual Thermodynamic Analysis of Turbulence – Part 1: Theory

M. Gustavsson*

Hot Disk AB, c/o Chalmers Science Park, Sven Hultins Gata 9, SE-41288 Gothenburg, Sweden
E-mail: Mattias.Gustavsson@hotdiskinstruments.com

Received 1 November 2021, Revised 14 March 2022, Accepted 24 March 2022

Abstract

A new theoretical groundwork for the analysis of wall-bounded turbulent flows is offered, the application of which is presented in a parallel paper. First, it is proposed that the turbulence phenomenon is connected to the onset of an irreversible process – specifically the action of a slip flow – by which a new fundamental model can be derived. Fluid cells with specific dimensions – of length connected with the local slip length and thickness connected with the distance between two parallel slipping flows – can be hypothetically constructed, in which a specific kinetic energy dissipation can be considered to occur. Second, via a maximum entropy production process a self-organized grouping of cells occurs – which results in the distinct zones viscous sublayer, buffer layer, and the log-law region to be built up. It appears that the underlying web structure may take the form of either representing a perfect web structure without any visible swirls, or a partially defect web structure where unbalanced forces may result in the generation of apparent swirls – which in turn might grow into larger turbulent eddies. Third, on the transition from laminar to turbulent flows, a nominal connection between the onset of a turbulent wall boundary layer (in a pipe flow), the Reynolds number as well as the wall surface roughness can be derived.

Keywords: *Discrete slip flow; maximum entropy production; turbulent eddy; fracture structure.*

1. Introduction

The topic of turbulence covers a broad range of experiments and attempts to analyse the phenomenon [1], [2], [3], [4], [5], [6]. The vastness of applications and results does not allow for any comprehensive summary in this paper.

However, most scientists within the field of turbulence would agree on the following points:

- Analysis of turbulent flows in simple geometries (pipes, plates etc.) is possible with empirical formulas. This is the default engineering approach [1].
- Wind tunnel experiments and scaling of results are a useful complement to empirical or numerical analysis in *e.g.* the aerospace and automobile industries. Corresponding experiments and scaling of results regarding marine- or submarine vessels is also possible in *e.g.* water channel experiments [2].
- Most attempts to model turbulence in a CFD (Computational Fluid Dynamics) flow solver employs the Navier-Stokes relations directly [7], or a modified- or altered version of these relations [3].
- The theory of a turbulent cascade process [8] is presumed, in which larger eddies are broken up downstream into smaller ones. The idea is to connect eddies to the concept of "turbulent kinetic energy", where the largest eddies are considered to have the highest amount of turbulent kinetic energy. After a cascade breakdown of eddies, eventually to the smallest scales (the Kolmogorov scales [9]), any further breakdown is the conversion into viscous dissipation.
- Perhaps the most ambitious computational-intense approach is the DNS (Direct Numerical Simulation) approach [7], [10], computing the time-dependent solutions of the flow utilizing the unaltered Navier-Stokes relations. Unfortunately, when modelling a situation where turbulence has triggered and is growing downstream (*e.g.* in a turbulent wall boundary layer), the corresponding DNS simulations hitherto arrive at opposite results, *i.e.* showing a receding turbulence downstream [11].
- In the LES (Large Eddy Simulation) approach [12], a low-pass filtering of the Navier-Stokes relations removes the information from the small eddies. The impact of the small eddies on the solution is instead modelled, while the large-scale eddies are analysed with the unaltered Navier-Stokes relations. It is argued that this approach removes the need to resolve small flow- and time scales.
- The k-ε turbulence model [13] simulates the mean-flow behaviour. It incorporates expressions for the turbulent kinetic energy k, as well as expressions for the "rate of dissipation of turbulent kinetic energy" ε. The concept of "eddy viscosity" is introduced – representing a "property of the flow".
- Despite various approaches results in various degrees of success, it is generally acknowledged that from hitherto acquired knowledge, one is not yet able to predict turbulent fluid motion in detail.
- There is no clear definition of turbulence. Reference is often made to *a list of characteristics of fluid flow behaviour*, *cf. e.g.* [3], which all need to be met to characterise the flow as "turbulent".
- It is fair to state that our understanding of turbulence is rather limited.

Would a fundamentally different approach have potential merit? Arguably yes, if one would consider the following:

*Corresponding Author

- It is here believed that the use of Newton's viscosity law $\tau_{ij} = \mu\left(\frac{\partial U_i}{\partial y_j} + \frac{\partial U_j}{\partial y_i}\right)$ (for an incompressible and Newtonian fluid) [2], [14] as a fundamental model for turbulent flows can be contested.[1] Clearly, a replacement fundamental model would approach the analysis of turbulence in a different way.
- The non-linear *slip flow* process occurs at far-from-equilibrium conditions [15] and has a corresponding residual thermodynamic process formulation [16]. Often ordered structures (often referred to as "dissipative structures") may be created in connection with the initiation of such a residual process [15].
- A simple *fracture* model based on multiple, but vertically separated slip flows, can fully resolve the time-averaged velocity profile of the so-called *viscous sublayer*, the *buffer layer*, the *log-law region*, and *outer region* of a turbulent wall boundary layer [1], [2]. The total kinetic energy dissipation can be integrated and compared with corresponding experiments with a certain degree of agreement, *cf.* Table 1 and computations in [17] for pipe flows.
- The concept of *perfect* slips fracture structure, and *defect* slips fracture structure can be introduced, where the defect slips fracture structure is associated with a reduced kinetic energy dissipation. For a perfect slips fracture structure, which appears to represent the situation within the viscous sublayer, all flow downstream occurs parallel to the wall, with no experimental evidence of swirls initiating within this zone. In addition, the viscous sublayer can also be considered to represent a *saturated* kinetic energy dissipation zone. Considering the buffer layer and log-law region, swirls may initiate (which downstream may form turbulent eddies, *cf.* discussion below and in [17]). But these may form only at relatively few spot-wise positions within the flow, *i.e.*, the connection between visible turbulence would relate to the presence of defects in the fracture structure.

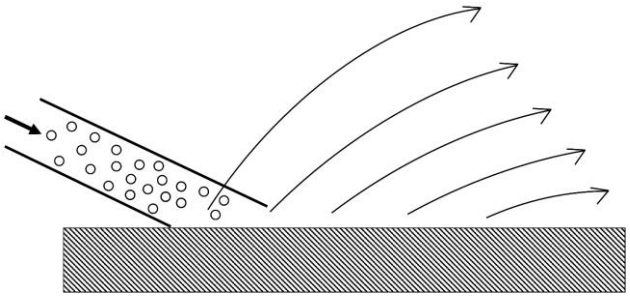

Figure 1. Impinging jet of round particles (erosives), impacting a ductile target surface, at an "initial state" of stationary conditions. Finnie and Kabil [18] characterised the reflected stream as "laminar".

In this paper, and in the associated paper [17], the discussion is focused on analysing the above-proposed model and evaluating it against experiments carried out on pipe channel flows.

Table 1. Comparison of traditional- versus proposed residual thermodynamic process approach.

Traditional approach on pipe cross-section:	Proposed approach on pipe cross-section:
$\overline{\mathbf{U}}_{\text{model}}$ does not agree with $\overline{\mathbf{U}}_{\text{experiment}}$ when solving the unaltered Navier-Stokes relations (in DNS simulations).	$\overline{\mathbf{U}}_{\text{model}}$ agrees with $\overline{\mathbf{U}}_{\text{experiment}}$, *cf.* [17].
$\mathbf{U}'_{\text{model}}$ in various degrees of agreement with $\mathbf{U}'_{\text{experiment}}$ (depending on alterations and artificial settings for closure when studying Reynolds decomposed Navier-Stokes relations).	$\mathbf{U}'_{\text{model}}$ considered to be of secondary importance.
Fundamental model: $\tau_{ij} = \mu\left(\frac{\partial U_i}{\partial y_j} + \frac{\partial U_j}{\partial y_i}\right)$ All irreversible thermodynamic processes occur close to equilibrium conditions, soft gradients.	Fundamental model: $\frac{\mathrm{d}(\mathrm{ke})_{\text{res}}}{\mathrm{d}t} = C_A \frac{\rho L}{\delta} U_{\text{slip}}$ valid at far-from-equilibrium conditions.
No specific triggering mechanism is presented in the turbulence sciences literature, to the author's knowledge.	Mechanism accounting for turbulence is believed to occur at far-from-equilibrium conditions and may trigger/onset at certain conditions.
1st law balance: No agreement yet claimed in the literature between model and experiments.	1st law balance: Agreement inferred.
2nd law balance: Not applicable (*cf.* incompressible flow assumption)	2nd law balance: Not applicable (*cf.* incompressible flow assumption)
Provides physical insight into origination of different zones in a turbulent wall boundary layer (viscous sublayer, buffer layer, and the log-law region): no.	Provides physical insight into origination of different zones in a turbulent wall boundary layer (viscous sublayer, buffer layer, and the log-law region): yes.
Connection surface roughness with analytical approach: not understood (the CFD modeller is referred to black-box model options).	Connection surface roughness with analytical approach: yes, experimental flow behaviour indicates effects to be accounted for when mapping the velocity profile.
The sciences of fluid dynamics have derived a closed set of equations, referred to as the non-altered set of Navier-Stokes relations for laminar flow. From a set of initial and boundary conditions, the Eulerian fluid flow field can be computed. Variants of this set of relations have been developed for analysis of turbulent flows. After a Reynolds decomposition, a set of relations can be derived without knowledge of all terms – the so-called "closure problem" of turbulence. These unknown terms need to be estimated (in a semi-empirical manner) to solve the set of equations.	To develop a closed set of relations solving the time-averaged Eulerian turbulent fluid flow field (including $\overline{\mathbf{U}}_{\text{model}}$), this remains to be developed (it is not the focus of the present work).

2. Theory

2.1 Preamble

Experimental observations made by [18] on a steady-state impinging dense particle-flow jet stream, resulting in erosion of a ductile material, is discussed. For round particles (so-called "erosives" within the field of Wear), impacting a

[1] In Capter 1.5 of [3] it is stated that "The Kolmogorov length and time scales are the smallest scales occurring in turbulent motion." – followed by a scientific argument concluding that continuum processes are the only possibility to consider for turbulent flows. The author of the present work believes that this argument is circular.

ductile target surface at relatively low impact angles, the initial behaviour when attacking a fresh target surface – not considering the first within 100 milliseconds or so when a "protective zone" [19] has not yet developed – behaves differently than later behaviour: At first, the net erosion rate is lower (which cannot be associated with any initial deviating surface material composition or oxide layer) than the net erosion rate observed later. Also, during this "initial state" the reflected flow is characterised as "laminar" [18]. As Finnie and Kabil were interested in the erosion behaviour of the target surface, they did not photograph or further characterise the reflection flow stream. However, Gustavsson [19] performed numerical simulations of an impinging 2D laminar particle-jet stream (at various flow conditions, width of jet, and impact angle against the target surface), *cf.* Figs 6-7 in [19]. These transient simulations were performed using a two-phase Eulerian-Eulerian flow solver [20], [21], [22]. For the impinging jet simulations, it was necessary to perform the simulations for a certain period (around a one-second simulation time), modelling the initial impact, followed by a build-up of a "protective layer" in the vicinity of the target surface, until eventually a steady-state flow condition was obtained, with results principally similar to the laminar flow situation depicted in Fig. 1, *cf.* [19].

Returning to the Finnie and Kabil experiments, after a "long-term" exposure of this steady-state impinging particle-flow jet stream of round erosives at relatively low impact angle, a regular pattern – a so-called "erosion ripple" pattern – would form in the target material. In addition, when ripples formed, it appeared that the net erosion rate was higher. For this later state, which we can refer to as the "state of erosion rippling", the observed reflected flow was characterised as "turbulent" [18], *cf.* Fig. 2.

The latter erosion ripple pattern formed on the target surface could be presumed to remain overly flat across the target surface, with the ripple wavelength representing typically a half- to full diameter of the erosives [18].

If one would consider modelling the turbulent flow of Fig. 2 in a two-phase Eulerian-Eulerian CFD flow solver involving only continuum models, an immediate complicating issue is that the erosion ripple wavelength is smaller than any envisioned continuum-length scale.

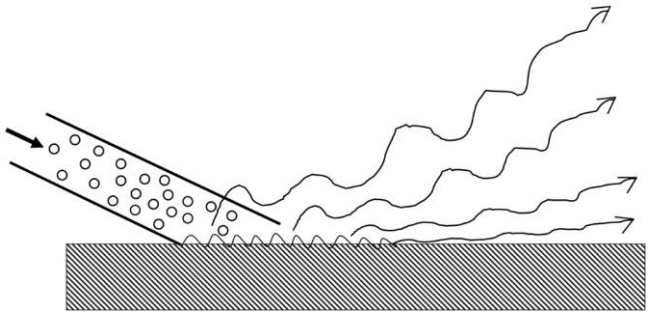

Figure 2. Impinging jet of round particles (erosives), impacting a ductile target surface, at a later state here referred to as a "state of erosion rippling". Finnie and Kabil [18] characterised the reflected stream as "turbulent".

Later, the tools of the residual thermodynamics framework [16] were employed to analyse the same case; First, the irreversible non-linear process of "ductile erosion" (the traditional description in the field of Wear) – or more precisely the irreversible process identified as "ductile wear" [23], [24] – was derived. Secondly, it was in [16] argued that the self-organisation of round erosives along the target surface through a "slip-roll" mechanism would result in ductile erosion, incorporating a geometrically fixed ripple wavelength pattern. The analysis of this case in [16] predicted ripple wavelengths close to- or in agreement with those observed in experiments.

The nominal slip-roll process resulting in erosion rippling was shown as possible to enhance by means of strengthened "dual-coupling" oscillation, *cf.* [16], *i.e.*, via further self-organisation of the effective thermodynamic forces and fluctuating thermodynamic flows. This enhancement – which is associated with an increase in the total residual entropy generation rate – results in increased net erosion rates.

Still, the net erosion rate is limited. Hence, for the net entropy generation around the entire impact zone of interest, it is fair to say that some kind of *maximization* of the net entropy generation (MEP = Maximum Entropy Production) appears to occur over time [25].

During this entire experiment, from onset of rippling through maximization, the nominal inflow jet stream is stationary and does not change with time.

Apparently, this self-organising behaviour occurs *outside* the target surface, hence this phenomenon occurs *within* the two-phase flow field (near the target surface). Consequently, this finding indicates that irreversible ***residual*** thermodynamic processes (*cf.* [16]) occur within the particle-gas or particle-vacuum flow field (*i.e.* outside the target surface) during the erosion rippling process.

In this paper, the observation by Finnie and Kabil [18] on characterising the reflected stream as turbulent is of interest to study further: When a turbulent reflective stream is at hand, this represents an outflow behaviour, which originates from an upstream condition in the flow field where one or several near-surface irreversible ***residual*** thermodynamic processes are acting, *cf.* Fig. 2. This, in contrast to the reflected stream being laminar when the outflow originates from an upstream condition in the flow field where only ***non-residual*** irreversible thermodynamic processes (*cf.* [16]) can be regarded as acting, *cf.* Fig. 1.

In other words, it appears not possible to model or simulate the "turbulent" flow situation in Fig. 2 utilizing only continuum models.

2.2 Appearance of Turbulence

Consider the physics in the immediate surroundings of the triggered slip-roll residual process resulting in erosion rippling in Fig. 2. According to [15] and [16], a continual supply of mechanical energy, or mass, or both combined, is required, in order to self-sustain the residual irreversible thermodynamic process (within the zone where $\mathrm{d_i}S_{\mathrm{res}} > 0$) above the onset condition. This supply comes from the immediate surroundings.

Next, consider a principal sketch of the immediate surroundings of the target surface subject to erosion rippling process, *cf.* Fig. 3.

The zone in which the discrete residual-process interaction accounting for ductile wear combined with erosion rippling is a certain zone stretching a certain distance from the wall itself, *i.e.*, the zone where $\mathrm{d_i}S_{\mathrm{res}} > 0$, *cf.* Fig. 3. This zone might have a different size in case erosion ripples have just begun to form, or when the erosion ripples reach their geometrical maximum amplitude (in other words, when overall net entropy generation has reached a maximum rate). Perhaps, the slip-rolling mechanism may not only

occur in the first 1-2 particle layers along the wall, but it may also influence the particle's organization – say 4-5 particle layers (or more) – outside the solid wall, *cf.* Figs 3-4.

If we choose to select the geometrical zone in which the slip-rolling mechanism creates a highly self-organized slip-rolling and entropy-generating zone, we can identify an exterior zone in which one is below the onset threshold for this residual process to enable – *i.e.,* within a non-residual thermodynamic condition $d_iS_{res} = 0$, *cf.* Figs 3-4.

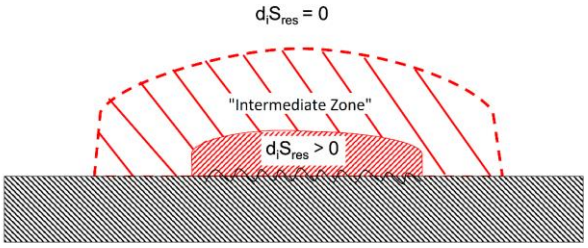

Figure 3. Principle separation of three different geometrical zones around the erosion ripples formed on the target surface. A zone with residual irreversible thermodynamic process, above onset threshold condition ($d_iS_{res} > 0$), with significant residual entropy generation (for a mechanical system), is present. This is the slip-roll process, possibly with some dual-coupling action. An exterior zone with sub-threshold conditions ($d_iS_{res} = 0$) can be identified, where no residual processes occur. Between these two zones, an "intermediate zone" can be imagined, which represents a geometrical zone in which both sub-threshold- or above-threshold conditions may exist for potential residual processes.

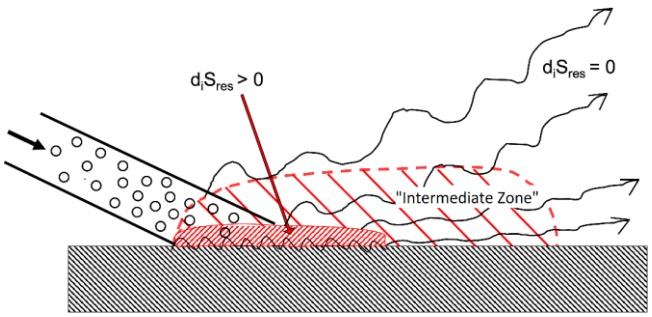

Figure 4. Author's estimation of zone sizes and locations (not to scale) for the three different geometrical zones – with fundamentally different physical behaviour in each of the respective zones – for the flow situation depicted in Fig. 2.

Between these two zones, we have an intermediate zone, *cf.* Figs 3-4. In this intermediate zone, which necessarily exists between the two extremes, one could reason that it would – for instance – represent a process condition A in Fig. 2 in [16]. In many instances in time and for most regions within this zone, one would be at sub-threshold conditions $d_iS_{res} = 0$, while for some instances in time and at certain regions within this zone, one would be at above threshold conditions $d_iS_{res} > 0$. Any fluctuations in thermodynamic forces may result in sudden entropy generation.

Such a process condition A is typically – according to [16] (with reference to experimental observations by Prigogine) – associated with high variations in concentrations, fluctuations etc., which might account for the downstream apparent "turbulent" behaviour of the reflected stream flow. Gustavsson states that (*cf.* below Table I in [16]): "However, fluctuations in the effective thermodynamic forces will render residual entropy generation for position A, where *dissipative structures appear as more chaotic and strong fluctuations in concentration can be induced*, …".

2.3 The Support Zone, and Connection with an Eddy, in The Erosion Ripple Jet Stream Flow

One may speculate on how the irreversible residual thermodynamic processes in the vicinity of the target surface (above the erosion ripple zone) interact with its nearest surroundings, and the behaviour of a possible locally-onset residual process at a position further downstream. In particular, ***the model envisions the <u>downstream leakage</u> of the residual-thermodynamic process zone, i.e., downstream extending of the zone*** $d_iS_{res} > 0$***, followed by breakage of the downstream-extended-zone*** $d_iS_{res} > 0$ **from the fixed erosion ripple region,** ***and continued lifetime of this residual process zone*** $d_iS_{res} > 0$ **as it moves** ***downstream*****.**

The downstream leaked – or broken-off – *R.Th.d.P.* (Residual-Thermodynamic Process) *zones* could be imagined as a thin, nonetheless extended in the downstream direction and yet with a significant width. Necessarily, the immediate surroundings will support this self-sustaining R.Th.d.P. zone with kinetic energy and possible mass flow from both sides, maintaining the onset condition of the downstream moving R.Th.d.P. zone.

The following experimental evidence supports this proposition:

1. The turbulent appearance of the reflected flow in Fig. 2 suggests that any given fixed geometrical position downstream of the onset residual-process zone $d_iS_{res} > 0$ might consist of either a sub-threshold condition $d_iS_{res} = 0$ or an above-threshold condition $d_iS_{res} > 0$ at different times.
2. A downstream moving broken-off R.Th.d.P. zone is necessarily surrounded by a much-larger *support zone*. In the following discussion, the R.Th.d.P. zone and associated support zone is referred to as a *turbulent eddy*, *cf.* Fig. 5. The concept of a turbulent eddy observed in experiments originally represent the size of coherent (or identifiable) structures observed in the flow. It is stated that eddies represent "packets" of fluid of different sizes (ranging from macroscopic to microscopic scales).
3. The maximisation of the net entropy generation in the entire impact zone appears to occur over time, after the residual thermodynamic process has been triggered to onset (for a stationary impinging particle jet flow). In order to maximize the net entropy generation, a downstream leakage of the onset process zone $d_iS_{res} > 0$ will occur.
4. As the natural behaviour tends towards maximising the net total entropy generation, after the onset of an erosion rippling process, it seems that one viable way to further increase the net total entropy generation, would be to self-organise additional life-support for these separated R.Th.d.P. zones as they move downstream. This maximization of entropy generation will possibly extend the length and/or width of the separated R.Th.d.P. zones, as well as extend the lifetime of the R.Th.d.P. zones as they move further downstream. This, in turn, would stretch the length of the "intermediate zone" yet further downstream, *cf.* Fig. 4.

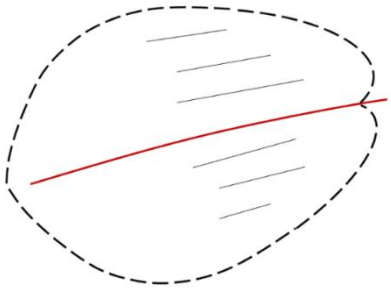

Figure 5. Consider an instantaneous condition: A geometrical zone supporting the above-threshold conditions to maintain onset of a separated discrete slip layer. In this paper, this supporting zone is referred to as a turbulent eddy.

Figure 5 depicts the possibility of an onset residual process (in red colour) that extends outside the specifically depicted turbulent eddy, into a connected turbulent eddy neighbour. At some point in time, these two co-joined turbulent eddies may break off from one another and reduce or increase in respective size.

The active R.Th.d.P. zone will reduce in size and the presence of R.Th.d.P. zones will cease to exist just prior to exiting the intermediate zone, *cf.* Fig. 4.

2.4 First Law Balance Relation Applied to a Single-Phase Turbulent Pipe Flow

We need an expression, allowing us to compute the Darcy friction factor from the total kinetic energy dissipation in a single-phase (nominally Newtonian fluid) pipe flow, valid for both viscous laminar and turbulent flows.

This can be obtained from the 1st law of thermodynamics, together with some common assumptions made in fluid dynamics of incompressible flows:

Consider a fully developed horizontal pipe flow (*i.e.*, no change in potential energy between inlet and outlet). Assume the fluid inside is incompressible, $v = 1/\rho =$ constant. Consider next an open system encompassing inlet to outlet, incorporating the fluid medium in the pipe. Assume in turn adiabatic conditions, $\dot{Q} = 0$, and no shaft work, $\dot{W}_{\text{shaft}} = 0$. Furthermore, assume steady state flow rate, $\dot{m} =$ constant.

We then obtain from the 1st law for open systems the following (valid for both viscous laminar- and turbulent flows):

$$\Delta \dot{E}_{\text{system}} = \underbrace{\dot{Q}}_{=0} - \underbrace{\dot{W}_{\text{shaft}}}_{=0} + (\dot{m}h)_{\text{in}} - (\dot{m}h)_{\text{out}} = 0 \tag{1}$$

where $h = u + Pv$ is the enthalpy.

The total kinetic energy dissipation is manifested as an increase in internal energy of the fluid at the outlet, minus inlet, multiplied by the mass flow rate. From Eq. (1) we get the following (valid for both viscous laminar- and turbulent flows):

$$\frac{\text{d(KE)}}{\text{d}t} = \dot{m}(u_{\text{out}} - u_{\text{in}}) = -\dot{m}v\Delta P = -\frac{\dot{m}\Delta P}{\rho} \tag{2}$$

Where we note that pressure change is negative (in the downstream direction) following thermodynamic sign conventions, and that the internal energy of the fluid leaving the pipe is higher than that of fluid entering the pipe, possible to record as an increase in temperature according to $\text{d}u = c_v \text{d}T$, *cf.* "incompressible flow" assumption in Section 2.10. Below, the fluid dynamic term pressure drop is discussed, a positive quantity, *i.e.*, pressure drop = $-\Delta P$.

In the following, it is important to keep track of whether assumptions and formulas relate to either viscous laminar flows, or turbulent flows.

Before connecting a new turbulence model to a pressure drop, it is a good first step to demonstrate that the outlined 1st law balance relations also apply for a viscous laminar flow. It is well-known from the fluid dynamics literature that there is an analytical connection between the Darcy friction factor (connected with pressure drop) and the Reynolds number for a fully developed laminar pipe flow of a Newtonian fluid.

Let us do the exercise of: Viscous laminar flow assumption → determine the kinetic energy dissipation locally (at radial positions in the pipe) from the linear fundamental model correlating shear stress, viscosity, and velocity gradients → integrating into total kinetic energy dissipation (which equals viscous dissipation) → via 1st law compute the pressure drop → allowing for estimation of the friction factor.

For a fully developed viscous laminar flow, with the above assumptions, we can from the Navier-Stokes expressions derive the pipe-downstream-direction velocity profile as:

$$U_1 = U_1(r) = U_{\max}\left(1 - \frac{r^2}{R^2}\right) \tag{3}$$

where R represents the radius of the pipe interior, and radius r stretches from the inner centreline $r = 0$ to $r = R$.

Also, the average-, or mean, flow speed for this viscous laminar case can be expressed as:

$$U_{\text{mean}} = U_{\max}/2 \tag{4}$$

From the fundamental model for viscous laminar flows, we have the connection $\tau = -\mu\frac{\partial U}{\partial r}$, where μ represents the dynamic viscosity of the Newtonian fluid.

According to fluid dynamic textbooks, the viscous laminar case gives us that the total kinetic energy dissipation in the pipe equals the integration of the viscous dissipation:

$$\frac{\text{d(KE)}}{\text{d}t} = \iiint \mu\left(\frac{\partial U_1}{\partial r}\right)^2 r\text{d}r\text{d}\theta\text{d}z \tag{5}$$

After a straightforward integration (using Eq. (3)) in the radial direction, and for all angles 0 to 2π, we obtain for the viscous laminar flow case:

$$\frac{\text{d(KE)}}{\text{d}t} = 2\pi\mu \int {U_{\max}}^2 \text{d}z \tag{6}$$

Using Eq. (4), and integrating over the entire pipe length section Z, we then obtain for the viscous laminar flow case:

$$\frac{\text{d(KE)}}{\text{d}t} = 8\pi\mu \cdot {U_{\text{mean}}}^2 \cdot Z \tag{7}$$

From Eq. (2), and the relation (valid for both viscous laminar- and turbulent flows):

$$\dot{m} = \rho\pi R^2 U_{\text{mean}} \tag{8}$$

we can directly compute the pressure drop for the viscous laminar flow case as:

$$\text{Pressure drop} = -\Delta P = \frac{8\mu \cdot U_{\text{mean}} \cdot Z}{R^2} \tag{9}$$

From Darcy's formula on pressure drop, the friction factor f is introduced (valid for both viscous laminar- and turbulent flows):

$$\text{Pressure drop} = f \cdot \frac{\rho Z \cdot {U_{\text{mean}}}^2}{2D} \tag{10}$$

Hence, inserting the pressure drop obtained for viscous laminar flows, Eq. (9), into Eq. (10), we can compute the dimensionless friction factor as:

$$f = \frac{64 \cdot \mu}{\rho \cdot U_{\text{mean}} \cdot D} = [\nu = \mu/\rho] = \frac{64 \cdot \nu}{U_{\text{mean}} \cdot D} = \left[\text{Re} = \frac{U_{\text{mean}} \cdot D}{\nu}\right] = \frac{64}{\text{Re}} \tag{11}$$

where ν represents the kinematic viscosity of the Newtonian fluid, and Re represents the dimensionless Reynolds number for pipe flows.

The friction factor, with above derivation, hence agrees with the friction factor as stated for viscous laminar flows in the fluid dynamics literature, *i.e.* $f = 64/\text{Re}$.

However, the traditional fluid dynamics derivation arriving at the same result was determined – instead of computing the total kinetic energy dissipation within the entire volume of the pipe – by computing the shear stress acting on solid walls. To illustrate:

From the surface wall shear stress acting on the cylindrical element surface, the parallel force defined by the wall shear stress (units N/m^2) multiplied by the area circumference multiplied by length of the cylinder $F = \tau_{\text{wall}} \cdot 2\pi R \cdot Z$, gives a pressure drop, which can be computed as $-\Delta P = F/A$, where $A = \pi R^2$. This gives (valid for both viscous laminar- and turbulent flows):

$$-\Delta P = 2\tau_{\text{wall}} Z/R \tag{12}$$

As the wall shear stress can be computed from $\tau_{\text{wall}} = \tau(r = R)$, we utilize the relationship for laminar flows $\tau = -\mu \frac{\partial U}{\partial r}$ and compute the derivative using Eq. (3), which gives us: $\tau_{\text{wall}} = 2\mu U_{\text{max}}/R$. Inserting this wall shear stress into Eq. (12) gives: $-\Delta P = 4\mu Z U_{\text{max}}/R^2$ for the viscous laminar flow case. Comparing this latter expression for laminar flows with the Darcy formula (Eq. (10)), we obtain the same result $f = 64/\text{Re}$ for the viscous laminar case. However, it is stressed that it is derived from Newton's laws of mechanics (not the 1st law of thermodynamics combined with a total integration of the total kinetic energy dissipation).

Hence, to compute the Darcy friction factor for turbulent flows Eq. (2) and Eq. (10) are used to compute the friction factor according to:

$$f = \frac{\left(\frac{\text{d(KE)}}{\text{d}t}\right)}{\dot{m}} \cdot \left(\frac{D}{Z}\right) \cdot \frac{1}{\frac{1}{2}(U_{\text{mean}})^2} \tag{13}$$

Note: Eq. (13) is valid for both viscous laminar flows as well as turbulent flows.

Our computational analysis work, in the following, will be to test our model, compute the net kinetic energy dissipation by integration, and compute the Darcy friction factor from Eq. (13). Hence, the proposed model can be compared to corresponding turbulent experiments – tabulated for turbulent pipe flows for different flow rates, surface roughnesses, pipe diameters, and fluid flow properties.

2.5 Single-Phase Turbulent Flows – Proposed Fracture Model and Fundamental Model

Unless otherwise stated, an Eulerian framework is adopted in the following.

The proposed web of fractures – assuming the MEP fracture model is active – is depicted in Fig. 6.

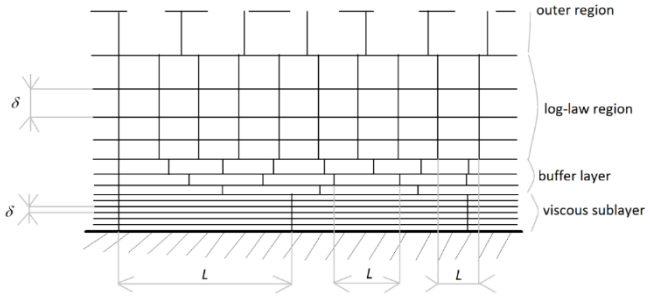

Figure 6. MEP fracture zone. In this 2D cross-section of the flow, assume Cartesian axis nr. 1 along the wall plane (in direction of the flow), and Cartesian axis nr. 2 perpendicular to the wall plane.

Assume that no velocity gradients exist between the fractures. The velocity of a flow parallel to a solid surface, $U_1(y_2)$, at a given y_2-position, is hence possible to determine by summation of the slip flow velocities from the solid surface to the y_2-position, where the corresponding resolution parameter δ (*cf.* Fig. 6) is summarized from the solid surface to the y_2-position. Thus, the experimentally recorded time-averaged velocities, and the stepwise discrete velocity variations, will closely match for a fine-enough resolution δ.

Considering the MEP process, the net kinetic energy dissipation is the highest possible if all kinetic energy dissipation occurs in the horizontal slips fracture zones, without presence of defects (and no swirls).

In this perfect fracture structure, without swirls, accounting for mass conservation or momentum conservation is not necessary. Blocks of fluid do flow downstream, at constant velocity.

In this fracture model, a first assumption is that the slip length L (considered a positive quantity in this work) correlates approximately linearly to the slip velocity U_{slip} (also considered a positive quantity in this paper):

$$L = C_B U_{\text{slip}} \tag{14}$$

Note: parameter L is finite, since an infinitely large L suggests an infinitely large U_{slip}, which is not possible.

Consider the conditions at a steady-state flow of parallel-positioned flakes, of thickness δ, of length L, and width K.

Consider a friction force acting on a slipping single flake, F_1, and assume a set of equidistant, and equally sized flakes of parallel flow, moving with the same relative slip flow U_{slip}. The friction force of a single flake can be replaced by a shear stress acting on the flake is $\tau = F_1/A = F_1/(K \cdot L)$, which gives a kinetic energy dissipation rate per unit volume $\text{d(ke)}_{\text{res}}/\text{d}t = \tau \cdot U_{\text{slip}}/\delta$ locally within the flow when ensemble averaging, due to this residual process.

A second assumption is that $\tau \propto U_{\text{slip}}$. From this, one may postulate: $\tau = C_A \cdot \rho \cdot C_B \cdot U_{\text{slip}}$, which gives:

$$\frac{\mathrm{d(ke)_{res}}}{\mathrm{d}t} = C_A \frac{\rho L}{\delta} U_{\text{slip}} \tag{15}$$

which represents a new fundamental model.

From a thermodynamic point of view, the entropy generation for this residual process can be expressed as: $\mathrm{d_i}S_{\text{res,gen}}/\mathrm{d}t = \left(G_{\text{proc}} - G_{\text{no proc}}\right) \cdot \mathrm{d}X/\mathrm{d}t$, *cf.* [16].

The work loss rate per unit volume resulting from this residual process can in turn be expressed as $|\delta w_{\text{res}}/\mathrm{d}t| = T \cdot \mathrm{d_i}s_{\text{res,gen}}/\mathrm{d}t$, where for this case $\mathrm{d_i}s_{\text{res,gen}}/\mathrm{d}t = \left(\mathrm{d_i}S_{\text{res,gen}}/\mathrm{d}t\right)/(K \cdot L \cdot \delta)$. This work loss rate also equals the kinetic energy dissipation rate, *i.e.* $\mathrm{d(ke)_{res}}/\mathrm{d}t = |\delta w_{\text{res}}/\mathrm{d}t|$.

From this, the corresponding effective thermodynamic force for this fracture model can be expressed (in units $\mathrm{J/(m^3K)}$) as:

$$G_{\text{proc}} - G_{\text{no proc}} = C_A C_B \cdot \rho \cdot \frac{L}{\delta} \cdot \frac{U_{\text{slip}}}{T} \tag{16}$$

and where the corresponding thermodynamic flow (in units $\mathrm{m^3/s}$) is $\mathrm{d}X/\mathrm{d}t = U_{\text{slip}} \cdot K \cdot \delta$.

A principally varying kinetic energy dissipation rate per unit volume (multiplied by $2\pi r \Delta r$) in an inner turbulent wall boundary layer is illustrated in Fig. 7.

Notwithstanding statements made in Section 2.3 and Fig. 5, the fracture model considers only the flake on one side of the slip process to act as support zone (or eddy). This perspective is adopted to simplify the computations, and to establish a well-defined L and δ, as well as K if the computations are to be made in 3D.

From a numerical point of view, a fine-enough resolution in δ will reduce errors occurring from this simplification.

2.6 Variation in L and δ, and The Presence of Defects

The presence of some non-symmetrical slip flows and/or some defects, will not automatically trigger or initiate a swirl. If the defects are large, or non-symmetry is considerable, then sometimes unbalanced forces may occur which results in the creation of a swirl.

Parameters L and δ can resolve and characterize an eddy: For instance, L and δ are invariant concepts connected with the instantaneous velocity vector, where a ***macroscopic eddy*** should be considered as a summation of flakes in the web fracture structure both lengthwise and crosswise, having a coherent motion. The parameters L and δ of a flake within a macroscopic eddy can be used to compute (or estimate) the local kinetic energy dissipation from Eq. (15).

Also, according to this proposed theory, the smallest-scale eddy, or the ***microscopic eddy***, would then be represented by the flakes defined by the parameters L and δ.

The MEP process acts to repair defects – maintaining the underlying fracture structure.

The ensuing web fracture structure is assumed to appear as follows:

1. The viscous sublayer has a constant $L = L_{\text{max}}$ and a constant $\delta = \delta = \delta_{\text{min}}$. The viscous sublayer can be considered to represent a saturated MEP fracture zone. Indeed, the constant L and constant δ across the viscous sublayer, indicates a constant kinetic energy dissipation across this viscous sublayer. Hence, it is assumed to represent a maximum state. Interestingly, when the surface roughness is increased, this maximum state zone is expanded in the $y_2{}^+$ direction (see below). Again, this experimental behaviour suggests that the viscous sublayer is a saturated MEP zone.
2. The buffer layer is simply an MEP fracture zone, linking the transition from the viscous sublayer zone to the log-law region. Turbulence scientists, albeit not discussing in terms of MEP behaviour, and not connecting their discussion to the present proposal, do indeed discuss the turbulent buffer layer as some kind of "transition" zone (of unclear definition) between the viscous sublayer and the log-law region. In the buffer layer, δ increases with increasing y_2. Simultaneously, the L parameter decreases with increasing y_2. The buffer layer is a zone which has a lot of "turbulence production", that is, the initiation of turbulent swirls, according to experiments. Indeed, if spreading out defects in this zone, and comparing with spreading out defects in the neighbouring viscous sub-layer zone, or in the log-law region, the non-symmetry will be highest in the buffer layer zone.
3. The log-law region has a fixed L (significantly smaller than in the viscous sublayer) throughout this region. However, δ increases with y_2. An important finding is that it can be mathematically shown that the log-law region, assuming the MEP fracture model, if applied all the way towards to the solid wall $y_2 = 0$, would correspond to integrating a kinetic energy dissipation expression corresponding to $1/y_2$ multiplied by a proportionality constant, which in turn if integrated all the way towards $y_2 = 0$ would tend to infinity. Since this is impossible, there is a position at a certain distance from the wall when the log-law region ceases to exist – which happens to be the position where the buffer layer ends, and the log-law region begins.

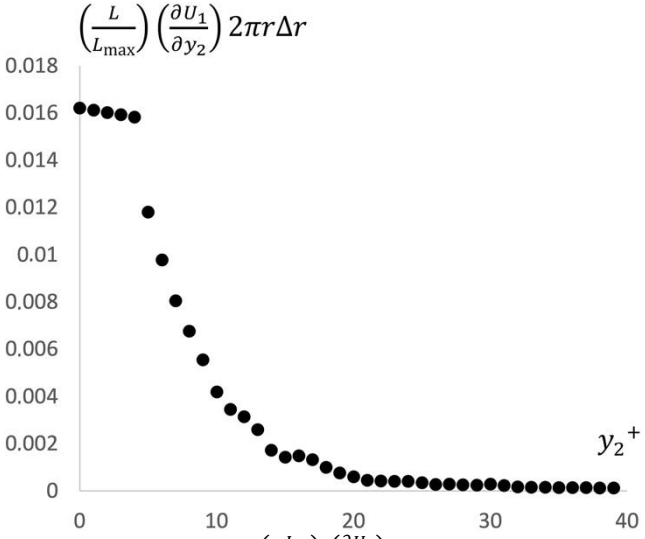

Figure 7. Variation of $\left(\frac{L}{L_{\max}}\right)\left(\frac{\partial U_1}{\partial y_2}\right)2\pi r\Delta r$ *vs.* $y_2{}^+$ *for the first case listed in Table 1 in* [17] *– cf.* Eq. (18) – where the resolution Δr is 1 wall unit. *Note the saturated (constant) kinetic energy dissipation in the viscous sublayer.*

In the outer layer, the web fracture structure breaks up almost immediately, and the presence of large swirly behaviour is present. The outer layer makes up approximately 80% of the entire thickness of the turbulent wall boundary layer, while the inner layers (viscous, buffer, and log-law) make up maybe around 20% of the total boundary layer thickness.

2.7 Accounting for The Surface Roughness

To evaluate the proposed model, the following two main considerations need to be addressed:

1. What can be said on the turbulent flow velocity profile variation with surface roughness? Traditional turbulence literature does not consider anything of importance to happen within the viscous sublayer zone. However, the implications in this paper (*e.g.* Fig. 7) as well as computations in [17], are that a considerable – if not the major – part of the net kinetic energy dissipation occurs within the viscous sublayer zone.

In experiments, the wall surface roughness does seem to have an impact. It increases the intercept value C of the log-law relation with increasing roughness. Also, some different sources suggest an ${y_2}^+$ thickness somewhere between 5 to 8 for the viscous sublayer. It is here proposed that an improved dimensionless correlation can be outlined between the non-dimensional flow ${U_1}^{++}$ and the non-dimensional position ${y_2}^{++}$ in accordance with Fig. 8, for the smoothest as well as for the roughest wall surface roughness. Any intermediate surface roughness can use Fig. 8 to compute interpolated variations of ${U_1}^{++}$*vs.* ${y_2}^{++}$.

Note that the proposed variations in ${U_1}^{++}$ *vs.* ${y_2}^{++}$ in Fig. 8 are by no means necessarily accurate, as there is little experimental data available today to back up the proposed variations. The maximum C^{++} in Fig. 8 could possibly be even higher, as well as the upper limit ${y_2}^{++} = 8$ thickness of the viscous sublayer thickness. Hopefully, future experimental studies can be made addressing this problem.

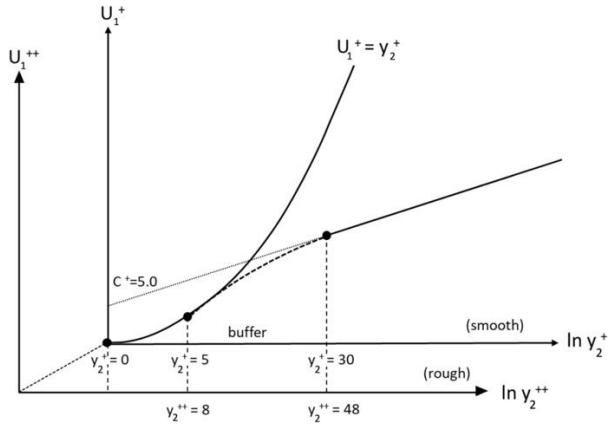

Figure 8. The non-dimensional velocity ${U_1}^{++}$ varies with ${y_2}^{++}$. In this figure is depicted the smoothest condition in accordance with ${U_1}^{++} = {U_1}^{+}$ and ${y_2}^{++} = {y_2}^{+}$ as depicted, or the viscous sublayer varies between ${y_2}^{++} = 0$ and ${y_2}^{++} = 5$, the buffer layer between ${y_2}^{++} = 5$ and ${y_2}^{++} = 30$. The log-law region is assumed valid for ${y_2}^{++} = 30$ to ${y_2}^{++} = 300$. The intercept in the log-law will then be around $C^{++} = 5.0$. For the roughest case, it is assumed that the viscous sublayer varies between ${y_2}^{++} = 0$ and ${y_2}^{++} = 8$, the buffer layer between ${y_2}^{++} = 8$ and ${y_2}^{++} = 48$, and the log-law region between ${y_2}^{++} = 48$ and ${y_2}^{++} = 300$. The intercept in the log-law will then be around $C^{++} = 7.0$. Any surface roughness between these two extreme states, the ${U_1}^{++}$ variation with ${y_2}^{++}$, as well as C^{++}, is obtained from a linear interpolation between these two extreme states.

2. What can be said on the fracture model variations of L and δ *vs.* y_2 – for different wall surface roughnesses?

Well, this question can be simplified in two steps:

First, it may be noted that if $U_{\text{mean}}({y_2}^+)$ and L are known, and the connection between U_{slip} and L is defined, *cf.* Eq. (14), then δ can be calculated. Hence, the following discussion need to only concern the variation of L *vs.* y_2 – for different wall surface roughnesses.

Second, since $L_{\max}$ may vary with surface roughness and the relevant flow conditions, it appears beneficial to work with a normalised $L = L(y_2)$:

$$L(y_2) = L_{max} \times \left(\frac{L}{L_{max}}\right)(y_2) \tag{17}$$

The implication that δ varies depending on the selection of L, suggests that the variation of L throughout a turbulent boundary layer can be modelled according to Fig. 9 for the smoothest- and roughest wall, respectively, where $L = L_{\max}$ at the solid wall.

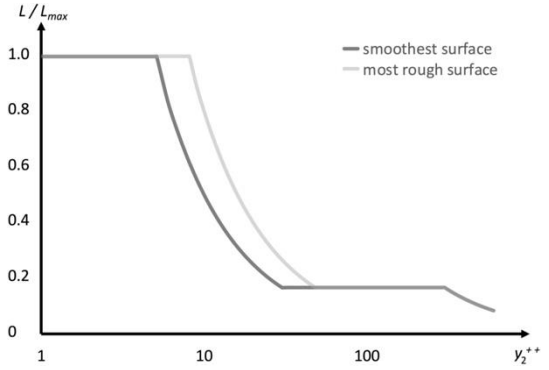

Figure 9. It is assumed that $L = L_{\max}$ throughout the viscous sublayer, and $L = L_{\max}/6$ throughout the log-law region. For the smoothest surface, ${y_2}^{++}$ will range between 0 and 5 in the viscous sublayer, and between 30 and 300 in the log-law region. For the roughest surface, ${y_2}^{++}$ will range between 0 and 8 in the viscous sublayer, and between 48 and 300 in the log-law region. In the buffer layer, it can be assumed that $L = 5L_{\max}/{y_2}^{++}$ for the smoothest surface, and $L = 8L_{\max}/{y_2}^{++}$ for the roughest surface. In the outer zone, in turn, it can be assumed that $L = 300L_{\max}/6{y_2}^{++}$.

2.8 Computations of Total Kinetic Energy Dissipation in Turbulent Pipe Flows

For a 1-meter pipe length ($Z = 1$ m), we connect directly the total kinetic energy dissipation to the volume integral of the local kinetic dissipation rate per unit volume, caused by the residual processes, according to:

$$\frac{\mathrm{d(KE)}}{\mathrm{d}t} = Z\int \frac{\mathrm{d(ke)_{res}}}{\mathrm{d}t} 2\pi r \mathrm{d}r = 1 \cdot \int C_A \frac{\rho L}{\delta} U_{\text{slip}} 2\pi r \mathrm{d}r \approx \int C_A \rho L \left(\frac{\partial U_1}{\partial y_2}\right) 2\pi r \mathrm{d}r = \rho C_A L_{\max} \int \left(\frac{L}{L_{\max}}\right)\left(\frac{\partial U_1}{\partial y_2}\right) 2\pi r \mathrm{d}r \tag{18}$$

where we immediately realize that $\left(\frac{\partial U_1}{\partial y_2}\right)(y_2)$ and $L(y_2)$ are known functions, *cf.* Figs 8-9.

When deriving Eq. (18), we utilize the approximation $\frac{U_{\text{slip}}}{\delta} \approx \frac{\partial U_1}{\partial y_2}$. This approximation is rather accurate, because where flow gradients are high, the fracture model requires a fine resolution of δ.

Furthermore, it is possible to replace L in Eq. (18) with the normalized L in Eq. (17), which allows the grouping of the terms $L_{\max}$, together with C_A and ρ, outside the integral.

From the above assumption, we can proceed computing the total kinetic energy dissipation, without information on the resolution, or C_B.

As regards the variation of kinetic energy dissipation per unit volume, in the different zones, or the net kinetic energy

dissipation associated with the fracture flakes, the following findings are important to note:

First finding: In the log-law region, we obtain:

$$\frac{L}{C_B\delta} = \frac{U_{\text{slip}}}{\delta} \approx \frac{\partial U_1}{\partial y_2} = \frac{1}{\kappa}\cdot\frac{U^*}{y_2} \tag{19}$$

where the only varying parameter on the left-hand side of Eq. (19) is δ, and the only parameter varying on the right-hand side is y_2 (the distance from the wall). Hence, if we would apply Eq. (19) in Eq. (18), and integrate all the way to the wall, the total kinetic energy dissipation would become infinite – which is not possible.

Second finding: It appears that for zones where L = constant, the net kinetic energy dissipation in the fracture flakes is equally large. That is, **in the viscous sublayer zone and log-law region, the net kinetic energy dissipation in the flakes is equal to the net kinetic energy dissipation of their neighbouring flakes in the y_2-direction**. In particular for the log-law region – where the kinetic energy dissipation rate per unit volume does decrease with increasing distance from the wall – the increasing flake size in the y_2-direction compensates for the decreasing kinetic energy dissipation rate per unit volume. This, in a way amounting to the product of flake volume and dissipation rate per unit volume, *i.e.* net kinetic energy dissipation rate, turns out equal in the y_2-direction.

2.9 Triggering of Turbulence

The fluid dynamics literature discusses the transition from viscous laminar flow to turbulent flow, *cf. e.g.* [2]. Influencing parameters are typically the Reynolds number, as well as the wall surface roughness (for boundary layer flow).

Other types of disturbances may also influence the onset of turbulence, such as a trip wire[2] positioned near the wall surface (positioned at or near the leading edge), or a sound wave. Normally, for a specific wall surface roughness, the transition to onset a turbulent wall boundary layer occurs at a specific Reynolds number. In case any artificially introduced disturbance such as a trip wire or an external sound wave is applied, the transition will occur at lower Reynolds numbers.

Observations have been made on turbulent spots [2] occurring near the solid wall just prior to the onset of the turbulent wall boundary layer. Some references argue that the concentration of these turbulent spots grow, and that when the concentration is large enough (effectively along the circumference of the inner pipe wall at a specific downstream position), the turbulent wall boundary layer triggers.

To analyse such transition theoretically, the principles of "linear stability analysis" – *cf.* [2] p. 673 – can be applied, where small disturbances are tested in linearized governing equations and boundary conditions. For a student of fluid dynamics, sometimes the concepts of discrete slip flow examples are encountered. For instance, for the "ideal slip flow" scenario (without any viscous processes occurring), it can be shown that disturbances of any wavelength (*cf.* [2] p. 679) may – under certain conditions – be amplified downstream. [This observation was utilized in the analysis of the erosion ripple process, where a connection between the erosion ripple wavelength and the slip-roll mechanism was proposed in [16].]

Equation (15) indicates that most of the net kinetic energy dissipation occurs within the viscous sublayer. This implies that a trip wire, sound wave or wall surface roughness directly influencing the viscous sublayer may have a significant influence on the onset of the turbulence process.

As is the case for the turbulence phenomenon, including the transition, the literature admits that the processes of transition from a laminar boundary-layer flow into a turbulent boundary layer flow is not fully understood.

However, to study the transition with the propositions made in this work – instead of analysing amplification of disturbances in linearized sets of equations – what if the transition would instead connect with a ***real*** process transition? Consider the transition of one active physical process (*e.g.* an irreversible process which is governed by the fundamental law for Newtonian fluids) resulting in laminar flow behaviour, to flip into another active physical process (*e.g.* an irreversible process which is governed by the here-proposed new fundamental model) which results in turbulence.

What would be suitable requirements for this process transition to occur?

Consider the following:

1. Apparently, it is required to occur at a specific geometrical position. (According to the residual thermodynamics dynamics framework, the geometry where transition/flipping may occur is typically rather limited, *i.e.*, the entire flow region will not instantaneously flip from a laminar flow process into a turbulent flow process.)

2. Probably the same (essentially) local kinetic energy dissipation for both processes would exist at this specific geometrical position. (Kinetic energy dissipation are key to the laminar flow relations, expressed as a viscous dissipation, while the kinetic energy dissipation is directly expressed in the here-proposed fundamental model for the slip-flow process, Eq. (15).)

3. The same essential flow conditions should also occur at this specific geometrical position, *i.e.*, the same flow gradients should pertain.

4. The process transition must occur in the vicinity of a solid wall, partly because when the velocity gradually increases, the viscous dissipation of the laminar flow increases until transition occurs, but also partly because the kinetic energy dissipation is the highest near the solid wall for the laminar flow, *i.e.*, the viscous laminar flow gradients are the highest in the vicinity of the solid wall.

From these conditions it is proposed that a turbulence transition analysis may be performed as follows:

First, the viscous laminar kinetic energy dissipation at the transition position can be expressed as:

$$\frac{\mathrm{d(ke)}}{\mathrm{d}t} = \frac{\mathrm{d(ke)_{viscous}}}{\mathrm{d}t} = \mu\left(\frac{\partial U_1}{\partial y_2}\right)^2 \tag{20}$$

At the same transition position, the proposed new fundamental relation gives the kinetic energy dissipation as:

$$\frac{\mathrm{d(ke)_{res}}}{\mathrm{d}t} = C_A\frac{\rho L}{\delta}U_{\text{slip}} \approx C_A\rho L_{\max}\frac{\partial U_1}{\partial y_2} \tag{21}$$

[2] The use of trip wires is sometimes valuable in experimental scaling work.

Equating these two expressions yields the following equation:

$$\mu\left(\frac{\partial U_1}{\partial y_2}\right)^2 - C_A\rho L_{\max}\left(\frac{\partial U_1}{\partial y_2}\right) = 0 \tag{22}$$

which gives the trivial solution $\frac{\partial U_1}{\partial y_2} = 0$, or $\frac{\partial U_1}{\partial y_2} = \frac{C_A\rho L_{\max}}{\mu}$.

For a pipe laminar flow, the velocity gradient $\frac{\partial U_1}{\partial y_2} = -\frac{\partial U_1}{\partial r}$ at the wall can be determined from Eq. (3). This gives the following nominal expression for the transition:

$$\frac{8{U_{\text{mean}}}^2}{C_A L_{\max}} = \frac{\rho U_{\text{mean}} D}{\mu} = \text{Re} \tag{23a}$$

For a pipe turbulent flow, the velocity gradient $\frac{\partial U_1}{\partial y_2}$ at the wall has an alternative formulation (in the viscous sublayer zone), *cf.* [17], which is: $\frac{\partial U_1}{\partial y_2} = \frac{(U^*)^2}{\nu}$. This gives, applying Eq. (10) and Eq. (12) the following alternative nominal formulation:

$$\frac{8C_A L_{\max}}{{U_{\text{mean}}}^2} = f \tag{23b}$$

Hence, Eq. (23a) presents a direct connection between the proposed new model and the Reynolds number at the turbulence onset transition point. Alternatively, Eq. (23b) presents a direct connection between $C_A L_{\max}$ and the Darcy friction factor f at the transition point.

Regarding these two expressions, Eqs (23a)-(23b), please note that the surface roughness and flow conditions influence the parameter $C_A L_{\max}$.

In [17], for a series of pipe cases, the proposed theory will be used to compute $C_A L_{\max}$.

2.10 Comments on The Incompressible Flow Assumption, and Prospects on a 2nd-law Balance

While the tools of residual thermodynamics and the 2nd law were pivotal in deriving a proposed new slip-flow process model and in identifying the proposed MEP processes, what else can be said on the application of the 2nd law on the present analysis?

Connecting with the developments of fluid dynamics, the assumption that the flow is incompressible (*i.e.*, the flow has constant density, viscosity, specific heat capacity and thermal conductivity) is made to simplify the derivations, and effectively separates the mechanical and thermal aspects of the flow (see [2], page 157).

According to [2], page 237, "The layman is usually surprised to learn that the pattern of the flow of air can be similar to that of water. From a thermodynamic standpoint, gases and liquids have quite different characteristics. As we know, liquids are often modelled as incompressible fluids. However, "incompressible fluid" is a thermodynamical term, whereas "incompressible flow" is a fluid-mechanical term. We can have an incompressible flow of a compressible fluid." Panton states that the main criterion for incompressible flow is that the Mach number be low ($M \to 0$). In addition, other criteria need to be fulfilled, *cf.* [2]. (Relating to this, all computations in [17] are performed for $M < 1/3$.)

While a general CFD flow solver analysis is based on the governing equations of fluid dynamics, continuity equation (conservation of mass), momentum equation (Newtons second law) and energy equation (conservation of energy), it was early in the present derivation stated that computations accounting for conservation of mass or momentum were not required for the analysis the time-averaged steady state turbulent flows in horizontal pipes. The focus was on the 1st law balance, and is the balance analysed in [17] for determination of model constants and evaluation of this approach.

How about a 2nd-law balance consideration?

The incompressible flow assumption appears to remove the need to consider a 2nd-law balance analysis in a regular CFD flow solver. It appears also to be the case here. In simple terms, the incompressible flow assumption makes a 2nd law net balance not meaningful to apply due to a lack of experimental data – a lack of data which anyway is not particularly important:

Consider, for instance, the following derived 2nd-law balance, reformulated as an expression of net entropy generation of water for a steady-state flow through a pipe:

$$\frac{\mathrm{d_i}S_{\text{gen}}}{\mathrm{d}t} = \sum \dot{m}(s_{\text{out}} - s_{\text{in}}) = \dot{m}c \cdot \ln\left(\frac{T_{\text{out}}}{T_{\text{in}}}\right), \tag{24}$$

where $c = c_v = c_p$.

The derivation assumes an adiabatic process, but generally, no experimental efforts have been made by fluid dynamists to arrange for an adiabatic process in the reference experiments. In addition, there appears to be no experimental data available on temperature increase of the water for reference pipe flows, to the author's knowledge (unless heat transfer is being analysed – a totally different field of science). This above expression assumes good mixing (which is the case for turbulent flows), *i.e.*, the same temperature across a pipe section inlet and outlet. It is immediately clear that it is not meaningful to apply a 2nd-law balance of the pipe flow, as there is no recorded experimental temperature data available to connect with.

A corresponding 2nd-law net balance for dry air (assumed to be an ideal gas) gives the following expression for the entropy generation of a steady-state flow through a pipe:

$$\frac{\mathrm{d_i}S_{\text{gen}}}{\mathrm{d}t} = \sum \dot{m}(s_{\text{out}} - s_{\text{in}}) = \dot{m}\left[\int_{T_{\text{in}}}^{T_{\text{out}}} c_p \frac{dT}{T} - \mathrm{R}_{\text{specific}} \cdot \ln\left(\frac{P_{\text{out}}}{P_{\text{in}}}\right)\right]. \tag{25}$$

Again, although experimental data is available on the pressure drop from reference experiments, there is no experimental data available on the temperature increase. Hence, again, it appears not meaningful to try to apply a 2nd-law balance analysis.

3. Discussion and Conclusions

The framework in [16], together with basic ideas of the Coulomb friction law, is utilized to derive a non-linear mechanism, associating slip flow with a kinetic energy dissipation rate. This serves as a new fundamental model, in a setting where the entire flow field is represented by a web of fractures. In accordance with [16], as this mechanism can be categorized as a residual irreversible thermodynamic process, the model coefficients in this new fundamental model do not represent any true material properties of the fluid.

It appears that the different zones (viscous sublayer, buffer layer and log-law regions) originating in the inner turbulent wall boundary layer does so, based on the action of

an overall MEP process occurring. Also, it appears that a downstream leakage[3] of slips appears to occur which appear to slightly increase the net kinetic energy dissipation rate downstream – implicating an overall slowly-evolving transient behaviour of turbulence, *cf.* [17].

The results indicate the highest net kinetic energy dissipation rates occurs in the viscous sublayer[4], followed by the buffer layer. The net kinetic energy dissipation appears to be somewhat limited in the log-law region, but still large enough to maintain an ongoing MEP process.

In addition, the present investigation proposes two alternative equations, where each of them indicates the transition condition from viscous laminar flows to the onset (or offset) of the slip flow fundamental model.

The large-scale eddies and swirls are solely distractors from the main processes occurring, having – as shown in [17] – little influence on the net kinetic energy dissipation rates.

On the matter of cascade theory, is there any equivalent such theory possible to apply for the present proposed theory? Perhaps not: While certainly kinetic energy can be estimated for a large-scale eddy, the matter of kinetic energy dissipation is more complex: While a small flake in the viscous sublayer, which is not associated with any turbulent behaviour or turbulent eddy, can have a much higher kinetic energy dissipation rate per unit volume as compared to a comparatively much larger flake (with large δ) within a large-scale turbulent eddy, it appears questionable to discuss kinetic energy dissipation of visible fluid structures, when these have a small contribution to the overall kinetic energy dissipation.

Finally, with the here-proposed onset of a slip-flow- and MEP process, the concept of turbulence can be physically and strictly well-defined.

Acknowledgements:

This work was supported by Hot Disk AB (Sweden). Special thanks to D.Sc. S.E. Gustafsson at Dept. Physics, Chalmers Univ. of Technology, Dr. H. Otterberg at University of Gothenburg, Assoc. Prof. J. Gustavsson and Prof. Å. Haglund at Dept. Microtechnology & Nanoscience, Chalmers Univ. of Technology, as well as Ms. B. Lee at Hot Disk AB (Sweden), for assistance in preparing this manuscript.

Nomenclature

A	area (m^2)
c	speed of sound in fluid ($m\ s^{-1}$)
C^+, C^{++}	log-law intercept on U^+- or U^{++}-axis, respectively (-)
C_A	model constant ($m\ s^{-2}$)
C_B	model constant (s)
c_p	specific heat at constant pressure ($J\ kg^{-1}\ K^{-1}$)
c_v	specific heat at constant volume ($J\ kg^{-1}\ K^{-1}$)
D	diameter of pipe interior (m)
K	flake width (in y_3-direction in Fig. 6) (m)
$\frac{\mathrm{d(KE)}}{\mathrm{d}t}$	total kinetic energy dissipation rate (W)
$\frac{\mathrm{d(ke)_{viscous}}}{\mathrm{d}t}$	viscous dissipation rate per unit volume ($W\ m^{-3}$)
$\frac{\mathrm{d(ke)}}{\mathrm{d}t}$	kinetic energy dissipation rate per unit volume ($W\ m^{-3}$)
E	energy (J)
F	force (N)
f	Darcy friction factor (-)
G	thermodynamic force (intensive unit)
h	specific enthalpy ($J\ kg^{-1}$)
L	slip length of flake (in y_1-direction in Fig. 6) (m)
M	Mach number, *e.g.* $M = U_{\mathrm{mean}}/c$ (-)
m	mass (kg)
$\dot{m}$	mass flow rate ($kg\ s^{-1}$)
P	static pressure ($N\ m^{-2}$)
Q	heat (J)
$\mathrm{R_{specific}}$	specific gas constant ($J\ kg^{-1}\ K^{-1}$)
R	radius of pipe interior (m)
r	radial distance from centerline (m)
Re	Reynolds number (-)
S	entropy ($J\ K^{-1}$)
s	specific entropy ($J\ kg^{-1}\ K^{-1}$)
T	absolute temperature (K)
t	time (s)
U	Velocity ($m\ s^{-1}$)
$\mathbf{U}$	velocity vector ($m\ s^{-1}$)
U_i	Cartesian component i of velocity vector ($m\ s^{-1}$)
U^*	Friction velocity, *cf.* [17] ($m\ s^{-1}$)
U_{max}	Maximum velocity ($m\ s^{-1}$)
U_{mean}	Mean (average) velocity ($m\ s^{-1}$)
U_{slip}	slip velocity ($m\ s^{-1}$)
u	specific internal energy ($J\ kg^{-1}$)
V	volume of flake fracture (m^3)
$v = \rho^{-1}$	specific volume ($m^3\ kg^{-1}$)
W	work (J)
$\lvert\delta w_{\mathrm{res}}/\mathrm{d}t\rvert$	work loss rate due to residual process ($W\ m^{-3}$)
X	thermodynamic flow (extensive unit)
y_1, y_2, y_3	Cartesian co-ordinates (m)
Z	pipe axis length of section (m)
z	length position in pipe axis direction (m)

Greek letters

θ	angle (between 0 and 2π) (-)

[3] *The net effect of the active MEP process is to slightly increase the net kinetic energy dissipation downstream*. The means at disposal for this is a complex re-arrangement of flakes (with respect to L and δ), mending "defect" slip layers, and likely extending slip lengths, possibly in combination with break-ups of slip layers, or by changing the number of slip layers. Hence the wording "leakage of slips".

[4] As the proposed theory suggests a stronger concentration of kinetic energy dissipation is shifted towards the wall – compared to the assumptions of traditional turbulence theory – it would be prudent to consider whether a high kinetic energy dissipation within the viscous sublayer, would result in increased local temperatures and adjusted local fluid properties? If so, what would be the effects? A ballpark estimation by the author for different fluids at $M < 1/3$ indicates that the primary behaviour would not be effected in a way which would directly overturn the proposed new theory, however there might be secondary phenomena that may result from the locally high kinetic energy dissipation.

δ	gap width between slip layers, also referred to as thickness of flake fracture, or resolution parameter (m)
κ	von Kármán constant, *cf.* [17] (-)
μ	dynamic viscosity of Newtonian fluid (kg m^{-1} s^{-1})
ν	kinematic viscosity of the Newtonian fluid (m^2 s^{-1})
ρ	density (kg m^{-3})
τ	shear stress (N m^{-2})
$\bar{\bar{\tau}}$	Cartesian shear stress tensor (N m^{-2})
τ_{ij}	components i, j of tensor $\bar{\bar{\tau}}$ (N m^{-2})

Subscripts

gen	generation
max	maximum
min	minimum
no proc	excluding specific sub-process of interest
proc	including specific sub-process of interest
res	for residual process
wall	wall position

Special notations

$\Delta(\cdot)$	difference
$\mathrm{d}(\cdot)$	differential [*e.g.* $\mathrm{d_i S_{res}}$ represents the differential entropy change due to residual process (J K^{-1})]
$\delta(\cdot)$	inexact differential
$\overline{(\cdot)}$	time average, used in Reynolds decomposition $\mathbf{U} = \overline{\mathbf{U}} + \mathbf{U}'$
$(\cdot)'$	fluctuating component, used in Reynolds decomposition $\mathbf{U} = \overline{\mathbf{U}} + \mathbf{U}'$
$\dot{(\cdot)}$	rate (s^{-1})
$\frac{\mathrm{d}}{\mathrm{d}t}, \frac{\delta}{\mathrm{d}t}$	time derivative (s^{-1})
$(\cdot)^{+}$	dimensionless scaling (traditional).
$(\cdot)^{++}$	dimensionless scaling – depending on the wall surface roughness.

References:

[1] F.M. White, *Fluid Mechanics*, 2nd Ed., McGraw-Hill Book Company, 1986.

[2] R.L. Panton, *Incompressible Flow*, John Wiley & Sons, New York, USA, 1984.

[3] H. Tennekes, J.L. Lumley, *A First Course in Turbulence*, MIT Press, 1972.

[4] P.A. Davidson, *Turbulence: An Introduction for Scientists and Engineers*, Oxford University Press, 2004.

[5] K. Sreenivasan, P.A. Davidson, Y. Kaneda, K. Moffatt, *A Voyage Through Turbulence*, Cambridge University Press, 2011.

[6] B. Herrmann, P. Oswald, R. Semaan and S. L. Bunton, "Modeling synchronization in forced turbulent oscillator flows", *Commun Phys 3:195*, 2020. DOI: 10.1038/s42005-020-00466-3.

[7] P. Moin, K. Mahesh, "DIRECT NUMERICAL SIMULATION: A Tool in Turbulence Research", *Annual Review of Fluid Mechanics 30*, 539-578, 1998.

[8] L.F. Richardson, *Weather Prediction by Numerical Process*, Cambridge University Press, 1922.

[9] A.N. Kolmogorov, "The Local Structure of Turbulence in Incompressible Viscous Fluid for Very Large Reynolds Numbers", *Proceedings of the USSR Academy of Sciences (in Russian), 30*, 299-303, 1941. Translated into English by L. Levin: A.N. Kolmogorov, "The Local Structure of Turbulence in Incompressible Viscous Fluid for Very Large Reynolds Numbers", *Proceedings of the Royal Society A, 434*, 9–13, 1991.

[10] C. Liu, P. Lu, L. Chen, Y. Yan, "New Theories on Boundary Layer Transition and Turbulence Formation", *Modelling and Simulation in Engineering*, Article ID 619419, 2012.

[11] R. Bose, P.A. Durbin, "Transition to Turbulence by Interaction of Free-Stream and Discrete Mode Perturbations", *Physics of Fluids 28*:114105, 2016.

[12] F. Ducros, P. Comte, M. Lesieur, "Large-Eddy Simulation of Transition to Turbulence in A Boundary Layer Developing Spatially Over a Flat Plate", *Journal of Fluid Mechanics, 326*, 1–36, 1996.

[13] B.E. Launder, D.B. Spalding, "The Numerical Computation of Turbulent Flows", *Computer Methods in Applied Mechanics and Engineering 3*, 269–289, 1974.

[14] Y. Demirel, *Nonequilibrium Thermodynamics: Transport and Rate Processes in Physical, Chemical and Biological Systems*, 3rd Ed., Elsevier, 2014.

[15] D. Kondepudi, I. Prigogine, *Modern Thermodynamics: From Heat Engines to Dissipative Structures*, Wiley, 1998.

[16] M. Gustavsson, ''Residual Thermodynamics: A Framework for Analysis of Non-Linear Irreversible Processes'', *Int. J. Thermodynamics, 15*, 69–82, 2012.

[17] M. Gustavsson, "A Residual Thermodynamic Analysis of Turbulence – Part 2: Pipe Flow Computations and Further Development of Theory", *submitted for publication*.

[18] I. Finnie, Y.H. Kabil, "On The Formation of Surface Ripples During Erosion", *Wear 8*, 60-69, 1965.

[19] M. Gustavsson, "Fluid Dynamic Mechanisms of Particle Flow Causing Ductile and Brittle Erosion", *Wear 252*, 845-858, 2002.

[20] H. Enwald, E. Peirano, GEMINI: A Cartesian Multiblock Finite Difference Code for Simulation of Gas-Particle Flows, Publikation Nr 97/4, Department of Thermo and Fluid Dynamics, Chalmers University of Technology, Sweden, 1997.

[21] M. Gustavsson, A.E. Almstedt, "Numerical Simulation of Fluid Dynamics in Fluidized Beds with Horizontal Heat Exchanger Tubes", *Chemical Engineering Science 55*, 857–866, 2000.

[22] M. Gustavsson, A.E. Almstedt, "Two-Fluid Modelling of Cooling-Tube Erosion in A Fluidized Bed", *Chemical Engineering Science 55*, 867–879, 2000.

[23] M. Gustavsson, "A Residual Thermodynamic Analysis of Inert Wear and Attrition, Part 1: Theory",

International Journal of Thermodynamics 18, 26-37, 2015.

[24] M. Gustavsson, "A Residual Thermodynamic Analysis of Inert Wear and Attrition, Part 2: Applications", *International Journal of Thermodynamics 18*, 39-52, 2015.

[25] A. Kleidon, Y. Malhi, P.M. Cox, "Maximum Entropy Production in Environmental and Ecological Systems", *Phil. Trans. R. Soc. B* 365, 1297-1302, 2010.